33RD CONGRESS
OF THE INTERNATIONAL COUNCIL
OF THE AERONAUTICAL SCIENCES
STOCKHOLM, SWEDEN, 4-9 SEPTEMBER, 2022

DESIGN OF STABILITY AUGMENTATION SYSTEMS FOR A FLEXIBLE AIRCRAFT USING LQ OUTPUT-FEEDBACK CONTROL VIA LMI

Renan L. Pereira[1], Pedro J. González[2] & Flávio J. Silvestre[3]

[1]Instituto Tecnológico de Aeronáutica
[2,3]Technische Universität Berlin

Abstract

This paper presents novel linear quadratic (LQ) output-feedback synthesis conditions for stability augmentation systems for flexible aircraft. The proposed conditions have been formulated using linear matrix inequalities (LMIs) to provide two different approaches: centralized and decentralized LQ with output-feedback framework. The main highlights of the present design conditions are the ability to obtain static LQ controllers for stability augmentation systems resorting only to weighting matrices as tuning parameters, as well as a straightforward condition for uncertain systems. In addition, such existence conditions may be a useful strategy due to the low complexity for practical controller implementations in flexible aircraft and demonstrators, such that improving aircraft handling qualities should be achieved. In order to demonstrate the effectiveness of the proposed strategies, a dynamic model of an unmanned remotely-piloted experimental airplane called X-HALE is adopted. Linear simulations are performed and the main procedure steps to obtain a realistic stability augmentation system are addressed.

Keywords: Flexible aircraft, LQ output-feedback control, Stability augmentation systems, LMIs.

1. Introduction

Flexible aircraft have received significant attention from the aeronautical community in recent years [1, 2]. One interesting feature of such aircraft are their high aspect ratio wings. They allow to increase the aircraft aerodynamic efficiency and reduce fuel consumption. As a result, a novel trend of aircraft with new lightweight structures and slender wings to reduce the aerodynamic drag has been designed [3]. This trend is noticed in state-of-the-art aircraft such as Boeing 787, Airbus A350, as well as the arising of high altitude long endurance (HALE) configurations. This unmanned aerial vehicles which are capable of flights for considerable periods of time without resort to landing, providing a low-cost alternative to surveillance purposes and low orbit satellites functions [4]. However, the operation and control of this aircraft class have proven to be a great challenge [5, 6]. The increase in flexibility leads to a coupling between the flight dynamics and the structural modes deteriorating the handling qualities characteristics of the aircraft [7]. In this case, the flight control law design for improving handling qualities has been one of the major problems since the guarantee of aeroservoelastic stability and performance should be achieved [8, 3].

Taking into account that the stability augmentation systems (SAS) allow enhancing the oscillatory dynamic stability of the aircraft in terms of a simple control loop, the search for static controllers has been an essential issue in the SAS design. Among all potential approaches, the one termed linear quadratic regulator with output-feedback proposed by [9] is undoubtedly a relevant technique applied by aeronautical practitioners in many engineering problems. This stems from the fact that the linear quadratic (LQ) output-feedback control gain found provides good robustness properties for the closed-loop system. A classical way to compute the LQ output-feedback gain for linear time-invariant (LTI) systems involves solving a Riccati equation in terms of an optimization routine given by Nelder and Mead through a simplex algorithm [10]. However, the standard formulation of this technique does not cope with uncertain linear systems, as well as it is necessary to provide the state initial condition to obtain feasible solutions, even knowing that for practical applications such assumption may be unrealistic. In addition, an initial stabilizing gain should also be selected to ensure the convergence of the algorithm. This assumption can be critical since flexible aircraft typically present high-order models [11].

In order to solve these shortcomings, to the best of our knowledge, this paper provides novel LQ output-feedback synthesis conditions, as well as a design procedure to obtain a SAS in a flexible aircraft called X-HALE [4, 11]. The proposed conditions have been formulated using a set of linear matrix inequalities (LMIs) [12, 13] to provide centralized and decentralized LQ output-feedback controllers through only the weighting matrices Q and R as tuning parameters. Herein the stability augmentation system designs are performed considering the linearized model of the X-HALE flexible aircraft around the straight and level flight condition with a given velocity and altitude. Moreover, two stability augmentation systems are addressed through just one design: a roll damper with feedback of roll rate to the aileron channel and a yaw damper with feedback of yaw rate to the asymmetric thrust channel.

This paper is organized as follows. Section 2 presents the flexible aircraft used to evaluate the SAS designs from the LQ output-feedback controllers obtained. Section 3 addresses the main contributions of this paper, where novel LMIs-based conditions for the LQ problem with output-feedback framework are derived. Section 4 illustrates the SAS design and results of the proposed method. Section 5 presents our conclusions.

The following notation is used throughout the paper. $\mathbb{R}^{n\times m}$ denotes the set of real $n \times m$ matrices. $\mathscr{M} > 0$ (or $\mathscr{M} < 0$) means $\mathscr{M}$ is symmetric and positive (or negative) definite. Tr$(.)$ is the trace of a matrix and **diag**$\{\dots\}$ is a diagonal matrix with the specified elements.

2. The X-HALE aircraft

The X-HALE aircraft is an unmanned remotely-piloted experimental airplane with very flexible wings that was originally designed and built by the University of Michigan (UMich) [4] to evaluate nonlinear aeroelastic phenomena and some control system designs [8, 3]. Since its conceptualization, other two prototypes were built in cooperation with the Instituto Tecnológico de Aeronáutica (ITA) and other funding agencies as FINEP (Financiadora de Estudos e Projetos) and EMBRAER (Empresa Brasileira de Aeronáutica) [11]. The first one is the X-HALE with four-meter-span configuration, it has a wing aspect ratio equal to 20 and is flexible, whereas the second airplane has six-meter-span configuration with aspect ratio equal to 30 and it is very flexible. In both configurations the central tail can be flipped in flight to either a horizontal or a vertical position to significantly modify the lateral-directional stability of the aircraft, more details about these configurations can be seen in [8, 3, 11]. In this paper, only the X-HALE with four-meter-span configuration will be considered (Figure 1).

Figure 1 – X-HALE with four-meter-span configuration.

2.1 Linear model description

The four-meter-span configuration X-HALE nonlinear model is based on the equations of motion derived for dually-constrained axes [14, 15]. In this mathematical formulation, the origin of the structural axes denoted by a material point without elastic displacement can be non-coincident with the origin of the body axes employed in the equation of motions. In this case, equilibrium points can be calculated leading to a model with all the structural degrees of freedom of the airplane. As a result, the modeling of the nonlinear flight dynamics around equilibrium yields to a reduced set of inertia-relieved constrained modes of vibration. Moreover, the aerodynamic model is given through the doublet-lattice method [16], where rational function approximations are applied to achieve the representation of aerodynamic loads possible in the time domain [17]. Hence, a significant number of aerodynamic lag states arise to make the approximation sufficiently accurate.

For the control design proposed, linear-time-invariant realizations from the nonlinear model under small disturbances around different equilibrium flight conditions can be obtained. In this case, the linear model description for the X-HALE with four-meter-span configuration can be represented as

$$G_{XHALE}:\begin{cases}\dot{x}(t)=A_{full}x(t)+B_{full}u_{full}(t)\\ y(t)=C_{full}x(t)+D_{full}u_{full}(t)\end{cases} \tag{1}$$

where $A_{full}\in\mathbb{R}^{219\times219}$ is the state matrix, $B_{full}\in\mathbb{R}^{219\times7}$ is the input matrix, $C_{full}\in\mathbb{R}^{114\times219}$ is the output matrix and $D_{full}\in\mathbb{R}^{114\times7}$ is the direct transmission matrix. For this model the state vector is given by

$$x=\left[\begin{array}{cccccccccccc|cccc} V & \alpha & q & \theta & h & x & \beta & \phi & p & r & \psi & y & \lambda_{rb}^T & \eta^T & \dot{\eta}^T & \lambda_\eta^T\end{array}\right]^T. \tag{2}$$

It is important to mention that this linear model includes the kinematic equations in the inertial reference frame for all six rigid-body degrees of freedom: displacements in the x and y directions, altitude h, and roll, pitch and yaw angles (ϕ, θ and ψ , respectively). Furthermore, the velocity V, the angle of attack α, the sideslip angle β, as well as the angular rates p, q and r also have their corresponding equations of motion. The modal amplitudes and their time derivatives are given by η and $\dot{\eta}$, respectively. Modes of vibration with frequencies up to 25 Hz are retained in the model [8, 3]. Aerodynamic lag states due to rigid-body and control-surface dynamics (λ_{rb}) and due to the aeroelastic dynamics (λ_η) are also incorporated.

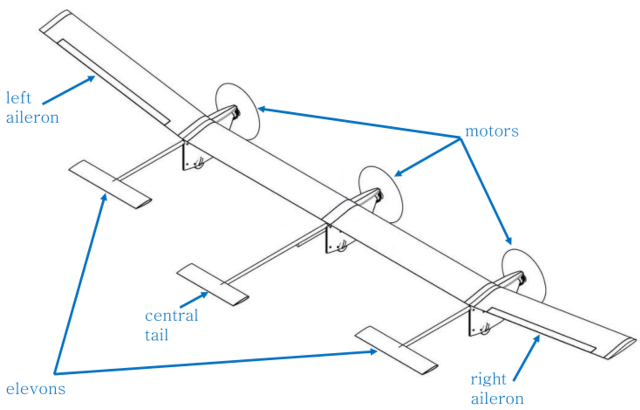

Figure 2 – Actuators description of the X-HALE with four-meter-span configuration.

In this context, the 219 states of the full linear model is composed by 12 states for denoted by the rigid-body motion $+$ 63 states for the rigid-body plus control-surface aerodynamic lag $+$ 32 for aeroelastic states and $+$ 112 states for aeroelastic aerodynamic lag. In addition, the X-HALE airplane has seven uncorrelated actuators distributed along two elevons ($\delta_{e(left)}$ and $\delta_{e(right)}$), two ailerons ($\delta_{a(left)}$ and $\delta_{a(right)}$) and three electric motors ($\delta_{throttle(left)}$, $\delta_{throttle(central)}$ and $\delta_{throttle(right)}$). As a result, the input vector can be written as

$$u_{full}=\left[\begin{array}{ccccccc}\delta_{a(left)} & \delta_{e(left)} & \delta_{e(right)} & \delta_{a(right)} & \delta_{throttle(left)} & \delta_{throttle(central)} & \delta_{throttle(right)}\end{array}\right]^T \tag{3}$$

and a diagram schematic for actuators description of the X-HALE with four-meter-span configuration may be depicted in Figure 2.
Moreover, associated with each actuator, a linear dynamic can be incorporated into the full linear model of the X-HALE to become the control design more effective. In this case, the control surfaces may be represented by a transfer function of first-order with a time constant of 48 ms and a transport delay of 60 ms, while the electric motor models may also be given by a transfer function of first-order with a constant time of 150 ms and the same transport delay value [3].

3. LQ output-feedback control via LMIs

In this section, LMI-based conditions to obtain static controllers for the LQ problem with output-feedback framework are derived. The synthesis conditions encompass the centralized control problem, as well as the decentralized approach. These conditions contain the main contributions of this paper.
Consider a strictly proper LTI system described in state-space form as

$$G_{yu}:\begin{cases}\dot{x}(t)=Ax(t)+Bu(t)\\ y(t)=Cx(t)\end{cases}\tag{4}$$

where $x(t)\in\mathbb{R}^{n}$, $u(t)\in\mathbb{R}^{n_u}$ and $y(t)\in\mathbb{R}^{n_y}$ are, respectively, the state vector, control input and measured output of the system. Herein the direct transmission term is supposed to be null, since many real-world problems can be modeled by plants with such characteristics. Moreover, it is assumed that (A,B,C) is stabilizable and detectable in order to ensure the sufficient conditions that allow to stabilize the open-loop system by static output-feedback controllers [18].
As it is well-known in the control literature, the linear quadratic (LQ) problem can be defined by minimization of the following performance index:

$$\begin{aligned}&J(x(t),u(t))=\frac{1}{2}\int_{0}^{\infty}\left[x^{T}(t)Qx(t)+u^{T}(t)Ru(t)\right]dt\\&s.t\\&\dot{x}(t)=Ax(t)+Bu(t)\end{aligned}\tag{5}$$

where the weighting matrices $Q\geq 0$ and $R>0$ [19, 20]. However, different from the state-feedback control approach widely presented in the literature, the present paper takes into account the output-feedback control law given by

$$u(t)=Ky(t),K\in R^{n_u\times n_y},\tag{6}$$

subject to LTI system denoted by (4). In this case, the LQ problem with output-feedback structure can be rewritten as

$$\begin{aligned}&J(x(t),u(t))=\frac{1}{2}\int_{0}^{\infty}x^{T}(t)\left[Q+C^{T}K^{T}RKC\right]x(t)dt\\&s.t\\&\dot{x}(t)=(A+BKC)x(t)\end{aligned}\tag{7}$$

As a consequence, the design problem consists in determining a static output-feedback controller K such that the cost function $J(.)$ is minimized. It is worth mentioning that the general static output-feedback control problem still is an unsolved problem [21]. A comprehensive survey on static output-feedback problem can be found in [22]. In other words, some assumptions must be considered to obtain feasible design conditions. These assumptions will be clarified throughout this section.
Now applying the property of the trace operator $Tr(\cdot)$ given by $\tilde{a}^{T}\mathscr{M}\tilde{b}=Tr\left(\mathscr{M}\tilde{b}\tilde{a}^{T}\right)$, with $\tilde{a},\tilde{b}\in\mathbb{R}^{n}$ and $\mathscr{M}\in\mathbb{R}^{n\times n}$, the quadratic performance index $J(.)$ defined in (7) can be recast as

$$J(x(t),u(t))=\frac{1}{2}\int_{0}^{\infty}Tr\left\{\left[Q+C^{T}K^{T}RKC\right]x(t)x^{T}(t)\right\}dt=Tr\left\{\left[Q+C^{T}K^{T}RKC\right]P\right\}\tag{8}$$

where $P=\frac{1}{2}\int_{0}^{\infty}\left[x(t)x^{T}(t)\right]dt$ is a definite positive symmetric matrix [23, 24, 20]. Therefore, a necessary and sufficient condition to ensure the stability of the closed-loop system for all evolution $x(t)$ can be posed such that

$$(A+BKC)P+P(A+BKC)^T+x_0x_0^T<0 \tag{9}$$

where x_0 denotes the initial condition of the open-loop system (4). In this sense, the LQ problem with output-feedback can be now rewritten as

$$\begin{aligned}&\min_{P,K} Tr(QP)+Tr\left(C^TK^TRKCP\right)\\ &s.t\\ &(A+BKC)P+P(A+BKC)^T+x_0x_0^T<0\end{aligned} \tag{10}$$

It can be seen that the currently problem (10) is not an LMI optimization problem, due to nonconvex terms, i.e. the unknown variables P and K are coupled. In order to solve this problem, additional mathematical manipulations should be done. In this case, taking into account the cyclic property of the trace operator in (10), we get

$$Tr\left(C^TK^TRKCP\right)=Tr\left(PC^TK^TRKC\right)=Tr\left(KCPC^TK^TR\right) \tag{11}$$

and knowing that the trace operator is invariant to similarity transformations, one may multiply the argument in (11) to the left by $R^{1/2}$ and to the right by $R^{-1/2}$ such that

$$Tr\left(KCPC^TK^TR\right)=Tr\left(R^{1/2}KCPC^TK^TR^{1/2}\right). \tag{12}$$

However, even doing such manipulations, the variables K and P still are coupled. Then using the Schur complement [12, 13], we obtain

$$X-R^{1/2}KCPC^TK^TR^{1/2}>0 \Leftrightarrow \begin{bmatrix} X & R^{1/2}KC \\ C^TK^TR^{1/2} & P^{-1}\end{bmatrix}>0 \tag{13}$$

where X is an upper bound matrix for the $Tr(.)$. Now, multiplying (13) by **diag**$\{I,P\}$ on the left and its transpose on the right, results in

$$\begin{bmatrix} X & R^{1/2}KCP \\ PC^TK^TR^{1/2} & P\end{bmatrix}>0. \tag{14}$$

It can be noticed that the variables K and P in condition (14) have the same arrange for stability condition derived in (9). As a result, we can use the W-strategy proposed by [25] to provide sufficient conditions for synthesis of static output-feedback controllers. Thus, the following theorem addresses a useful solution for the LQ problem with output-feedback.

Theorem 1 *Consider the LTI system described in* (4) *subject to cost function* (8)*. For given weighting matrices $Q\geq 0$ and $R>0$ and initial condition x_0. There exists a static output-feedback gain $K=NM^{-1}$, if there exist the matrices $N\in\mathbb{R}^{n_u\times n_y}$, $M\in\mathbb{R}^{n_y\times n_y}$ and symmetric matrices $P>0\in\mathbb{R}^{n\times n}$ and $X\in\mathbb{R}^{n_u\times n_u}$ that solve the following LMI optimization problem:*

$$\begin{aligned}&\min_{P,N,M,X} Tr(QP)+Tr(X)\\ &s.t\\ &\begin{bmatrix} X & R^{1/2}NC \\ C^TN^TR^{1/2} & P\end{bmatrix}>0,\ MC=CP,\\ &AP+PA^T+BNC+C^TN^TB^T+x_0x_0^T<0\end{aligned} \tag{15}$$

Proof 1 *Taking into account that C is full row rank, then the change of variable $MC=CP$ is guaranteed because M is positive definite. Thus using an output-feedback gain $K=NM^{-1}$, the conditions* (9) *and* (14) *are recovered for the closed-loop system $A_{cl}=A+BKC$. Hence, the proof is complete.*

Remark 1 *Notice that a reservation of the synthesis condition proposed is that C be full row rank. However, such limitation may be overcome using an appropriate similarity transformation, please see [26]. In addition, adopting $C=I_n$ as full-information case, the state-feedback control condition derived in [20] may be recovered, as well as the change of variable $MC=CP$ becomes redundant. Finally, the other reservation about the Theorem consists in the difficulty of satisfying the equality constraint $MC=CP$ since the output matrix may have elements that do not allow commutation.*

Remark 2 *It can also be seen that a straightforward extension for uncertain systems can also be obtained. In this case, a guaranteed cost controller with output-feedback is achieved.*

Given Theorem 1, it is also possible to obtain a decentralized synthesis condition, in which will be employed in this paper. It is well-known in aeronautical applications that such strategies can be useful. The motivation stems from the fact that for some conditions, the aircraft longitudinal dynamics can be treated as decoupled of the lateral dynamics, aiding the control design. In this sense, a decentralized LQ output-feedback condition from Theorem 1 may be derived as follows.

Corollary 1 *Consider the LTI system described in* (4) *subject to cost function* (8)*. For given weighting matrices* $Q \geq 0$ *and* $R > 0$ *and initial condition* x_0*. There exists a decentralized output-feedback gain* $K = NM^{-1}$*, if there exist the matrices* $N = diag\{N_1, ..., N_N\} \in \mathbb{R}^{n_u \times n_y}$*,* $M = diag\{M_1, ..., M_N\} \in \mathbb{R}^{n_y \times n_y}$ *and symmetric matrices* $P > 0 \in \mathbb{R}^{n \times n}$ *and* $X \in \mathbb{R}^{n_u \times n_u}$ *that solve the following LMI optimization problem* (15)*.*

Given the LMI-based conditions provided, two alternative stability augmentation system designs, centralized and decentralized, can be performed in the X-HALE aircraft. For each controller configuration, a roll damper with feedback of roll rate to the aileron channel and a yaw damper with feedback of yaw rate to the rudder channel will be provided using just one SAS design. The main procedure steps are addressed in the next section.

4. Design procedure and results

This section addresses two stability augmentation system designs using LQ output-feedback controllers. The first one consists in determining a centralized controller using the LMI-based conditions provided in Theorem 1, while the second design deals with the synthesis of a decentralized output-feedback controller denoted in Corollary 1. In order to evaluate such synthesis conditions, the same weighting matrices and initial conditions are considered.

4.1 SAS design and model order reduction

The stability augmentation system designs are performed considering the linearized model of the X-HALE flexible aircraft around the straight and level flight condition with velocity of 16 $[m/s]$ and altitude of 650 meters, as well as all aircraft actuators can be independently controlled. In this case, it is adopted that the rolling motion is controlled by the ailerons $\delta_{a(left)}$ and $\delta_{a(right)}$ operating anti-symmetrically $(\delta_{a(left)} = -\delta_{a(right)})$, whereas the yawing motion is controlled using differential throttle of the external motors $(\delta_{throttle(right)} - \delta_{throttle(left)})$, yielding a rudder movement. As a result, the input control vector can be denoted by

$$u(t) = \begin{bmatrix} \delta_a \\ \delta_r \end{bmatrix} = \begin{bmatrix} \delta_{a(right)} \\ \delta_{throttle(right)} - \delta_{throttle(left)} \end{bmatrix} \tag{16}$$

where the input signal $u(t) \in \mathbb{R}^{2\times1}$. In this case, the input matrix used for the SAS designs can be formulated as

$$B_{SAS} = \left[\begin{array}{c|c} B_4 - B_1 & B_7 - B_5 \end{array} \right] \tag{17}$$

and the direct transmission matrix as

$$D_{SAS} = \left[\begin{array}{c|c} D_4 - D_1 & D_7 - D_5 \end{array} \right] \tag{18}$$

where B_j represents the j-th column of the full input matrix $B_{full} \in \mathbb{R}^{219\times7}$ and D_j the j-th column of $D_{full} \in \mathbb{R}^{114\times7}$. As a consequence, the linear state-space model employed in the SAS design can be cast as

$$G_{SAS} : \begin{cases} \dot{x}(t) = A_{full}x(t) + B_{SAS}u(t) \\ y(t) = C_{full}x(t) + D_{SAS}u(t) \end{cases} \tag{19}$$

It can be seen that two stability augmentation systems are addressed through just one design : a roll damper with feedback of roll rate (p) to the aileron channel (δ_a) and a yaw damper with feedback of yaw rate (r) to the rudder channel (δ_r). Moreover, it is worth mentioning that although the evaluation of the SAS designs is done by the full model (19), the LMI synthesis conditions derived in Theorem 1 and Corollary 1 do not cope with high-order models. Thus a reduced X-HALE model to avoid numerical issues should be pursued. In this case, the balanced truncation method is employed. The first step to apply the balanced truncation method consists in evaluating the states contribution in terms of the Hankel singular values. These contributions are characterized by the decomposing of G_{SAS} into stable and unstable modes. In Figure 3, both stable and unstable modes of the full model in (19) can be interpreted from the eigenvalues of the controllability and observability gramians. From the stable

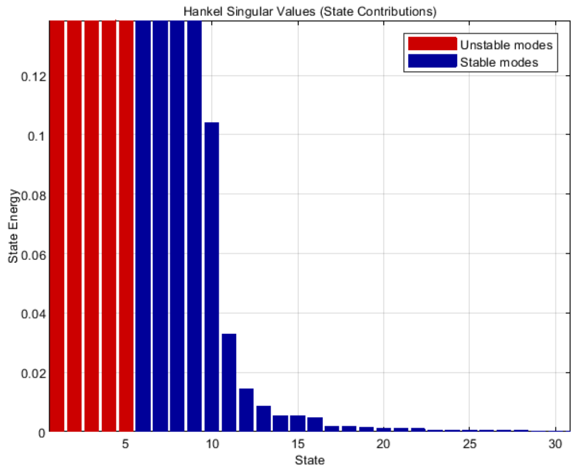

Figure 3 – Analysis of the stable and unstable modes using Hankel singular values.

and unstable modes analysis, the resulting reduced-order linear model comprises 8 rigid-body states (with x, y, ψ, and h discarded), 8 aeroelastic states, totalizing 16 states. By using the comparison between the maximum (σ_{max}) and minimum (σ_{min}) singular values obtained through both full-order and reduced-order linear models, we can notice that the reduced-order model is close enough to the full-order model (Figure 4). This stems from the fact that the truncation error can be calculated using

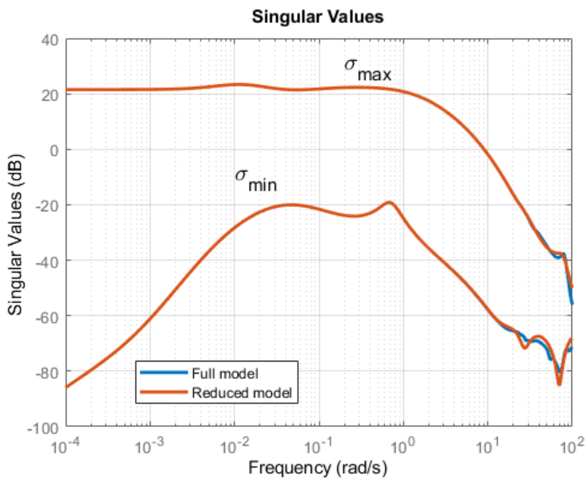

Figure 4 – Comparison between the maximum (σ_{max}) and minimum (σ_{min}) singular values of both full-order and reduced-order linear models.

the tail of the Hankel singular values, in which can be defined as

$$\left\|G_{SAS} - \hat{G}_{SAS}\right\|_{\infty} \leq 2\left(\sigma_{r+1} + \sigma_{r+2} + \ldots \sigma_N\right), \tag{20}$$

where the reduced-order model is given by $\hat{G}_{SAS}$ and the $\|.\|_{\infty}$ belongs to induced $\mathscr{L}_{\infty}$ norm. Thus the truncation error is bounded by

$$\left\|G_{SAS} - \hat{G}_{SAS}\right\|_{\infty} \leq 0.0038. \tag{21}$$

Following the SAS design procedure, it is important to mention that the control law for both roll damper and yaw damper designs is built doing

$$u(t) = \upsilon(t) + u_{SAS}(t) \tag{22}$$

where $\upsilon(t)$ corresponds to pilot inputs and $u_{SAS}(t)$ the input of the SAS. Hence, we can obtain the appropriate formulation to employ the proposed strategies, in which a strictly proper plant should be assumed. In this sense, we get

$$u_{SAS}(t) = Ky_{SAS}(t) = KC_{SAS}\left[C_{full}x(t) + D_{SAS}u(t)\right] = KC_{SAS}C_{full}x(t) \tag{23}$$

where C_{SAS} is a Boolean matrix associated with outputs of interest, characterized by roll rate (p) and yaw rate (r). Finally, two stability augmentation system designs using LQ output-feedback controllers can be provided and evaluated. In this case, regarding centralized and decentralized synthesis conditions presented in Theorem 1 and Corollary 1, respectively.

4.2 Results

Herein the centralized and decentralized output-feedback gains found via the proposed syntheses conditions are presented, as well as the responses to aileron doublet input and rudder doublet input considering the vertical-central-tail X-HALE configuration at 16 $[m/s]$. In order to evaluate the effectiveness of the proposed strategies, the weighting matrices Q and R are chosen as $Q = 25\cdot 10^4 I_{16\times 16}$ and $R = 2.5\cdot 10^3 I_{2\times 2}$ for both designs. The synthesis described in this section was implemented using the following software suites: MATLAB® software, version 9.9.0 R2022b, Yalmip [27] and SeDuMi [28].

4.2.1 Centralized SAS design

By using the Theorem 1 for initial condition null and the correspondent weighting matrices defined above, we can obtain the matrices N and M that recover the centralized LQ output-feedback gain K_c given by

$$K_c = \underbrace{10^{-7}\begin{bmatrix} 0.6253 & 0.2158 \\ 0.0530 & 0.0293 \end{bmatrix}}_{N} \underbrace{10^{7}\begin{bmatrix} 1.9402 & -0.1352 \\ -5.3354 & 0.6416 \end{bmatrix}}_{M^{-1}} = \begin{bmatrix} 0.0618 & 0.0539 \\ -0.0537 & 0.0117 \end{bmatrix}, \tag{24}$$

in which can be used to evaluate the closed-loop system performance in comparison to the open-loop

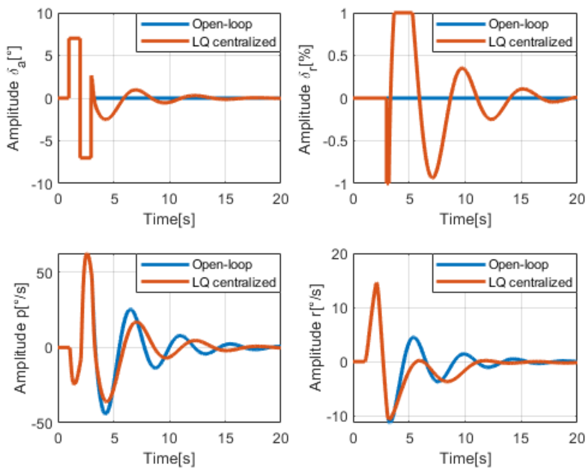

Figure 5 – Response to the 7-degree aileron doublet input (Centralized).

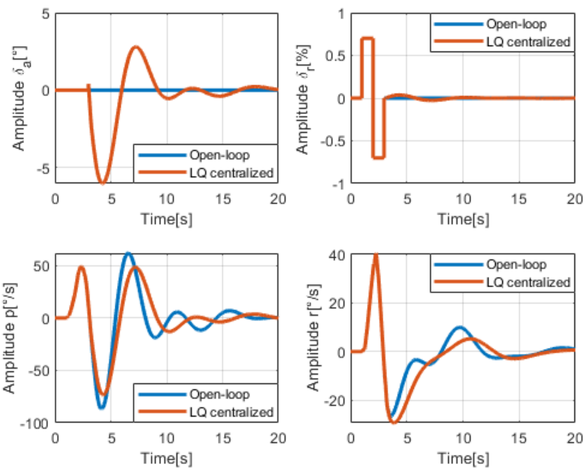

Figure 6 – Response to the 70-percent rudder doublet input (Centralized).

system. For this comparison, the doublets in the aileron and rudder are applied while the control-loop is open (3 seconds). In this case, Figures 5 and 6 show that some improvements regarding the aircraft handling qualities in terms of overshoot, settling time, and reduction of the oscillation can be noticed. However, such improvements are given due to greater employment of the aileron and rudder deflections in relation open-loop system. An alternative solution to avoid these efforts consist in setting novel weighting matrices or using pre and post-compensators in the design. Although these points are major in practical terms, the idea of this paper is to provide alternative methods to design stability augmentation systems using a straightforward synthesis. In this sense, it follows the decentralized SAS design results for our X-HALE aircraft.

4.2.2 Decentralized SAS design

For the decentralized design, the Corollary 1 condition is used for the same initializing conditions, resulting in the following diagonal matrices N and M, in which are addressed to achieve the decentralized LQ output-feedback gain

$$K_d = \underbrace{10^{-7}\begin{bmatrix} 0.1763 & 0 \\ 0 & -0.0183 \end{bmatrix}}_{N} \underbrace{10^{6}\begin{bmatrix} 1.6989 & 0 \\ 0 & -4.6383 \end{bmatrix}}_{M^{-1}} = \begin{bmatrix} 0.0299 & 0 \\ 0 & 0.0085 \end{bmatrix}. \tag{25}$$

Taking into account the same analysis procedure done for the centralized SAS design, doublet-type commands are applied individually for a given amplitude to the aileron and rudder to stimulate the lateral-directional modes according to the open control loop in 3 seconds. Figures 7 and 8 show that a small improvement regarding the aircraft handling qualities in terms of overshoot, settling time, and reduction of the oscillation is obtained. However, the control efforts are reduced. In this sense, a fair comparison between the centralized and decentralized SAS designs may be made.
From simulations and the Figures 9 and 10, it can be seen that the linear results show that both SAS designs present satisfactory performances with respect to the lateral-directional modes since stabilizing and damped responses are achieved. Moreover, we can also notice that the centralized output-feedback synthesis requires greater control effort than the decentralized approach, reducing the lifespan of the actuator. However, it is worth mentioning that for the flexible X-HALE aircraft study case, the centralized SAS controller can be properly applied since the input signal of the actuator does not violate the physical limits of the aileron and rudder.

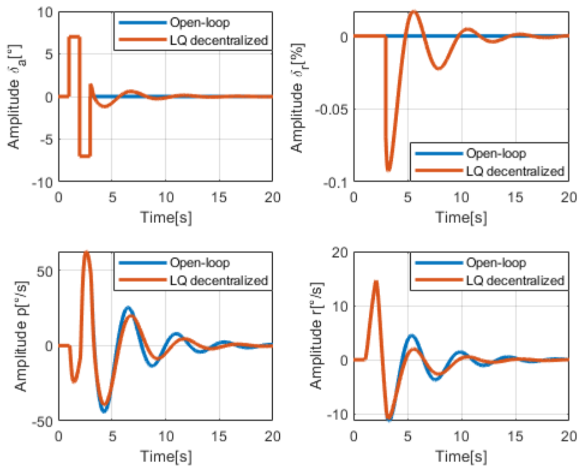

Figure 7 – Response to the 7-degree aileron doublet input (Decentralized).

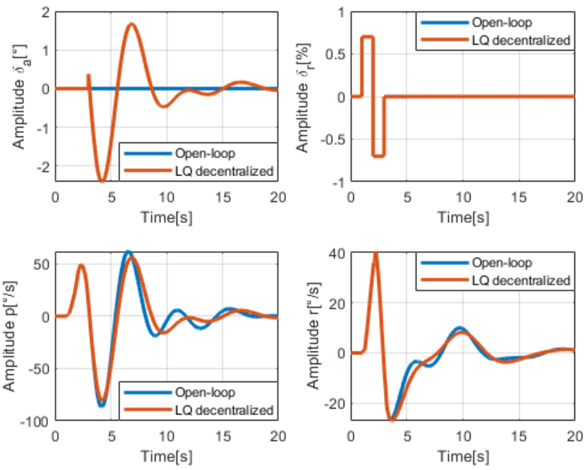

Figure 8 – Response to the 70-percent rudder doublet input (Decentralized).

In addition, another important criteria analysis beyond the responses in time is the robustness notion. In this case, we choose the disk margin concept to evaluate the robustness of the controllers designed [29]. The formulation arises from the small gain theorem, such that the peak gains of the complementary sensitivity $\mathbb{T}$ and sensitivity $\mathbb{S}$ functions can be employed. As the designed output

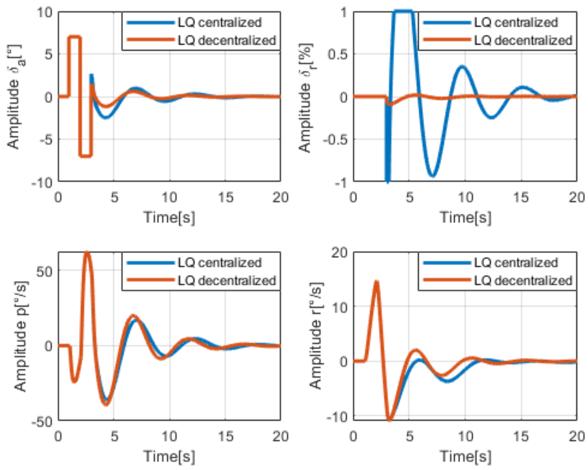

Figure 9 – Response to the 7-degree aileron doublet input.

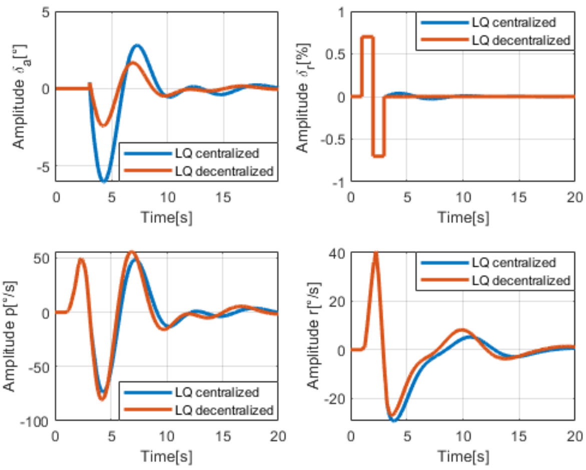

Figure 10 – Response to the 70-percent rudder doublet input.

feedback controllers guarantee the stability of the closed-loop system, the peak gains can be interpreted as the ∞ norm values of the sensitivities functions defined by

$$\mathbb{S} = (I + G_{SAS}K)^{-1} \text{ and } \mathbb{T} = (I + G_{SAS}K)^{-1} G_{SAS}K. \tag{26}$$

Therefore, adopting that there exists an uncertainty denoted by Δ between the output-feedback controller and the plant, an upper linear fractional transformation $F_u\left((\mathbb{S}-\mathbb{T})^{-1}, \Delta\right)$ may be applied such that the input disk margin notion corresponds to Figure 11.

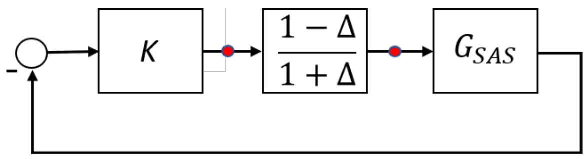

Figure 11 – Block diagram of the input disk margin concept.

As a consequence, the input disk margin framework is asymptotically stable if and only if

$$\|\Delta\|_\infty < \delta \Rightarrow \delta = \frac{1}{\|\mathbb{S}-\mathbb{T}\|_\infty}, \text{ for } 0 < \delta < 1. \tag{27}$$

In this case, the robustness analysis may be interpreted in terms of the Nyquist graph taking into account the distance of $G_{SAS}K$ to the origin or the point -1 for each input channel [29]. Due to this feature, some classical properties such as gain margins and phase margins can be used to measure the robustness of both controllers designed. As a result, the lower and upper disk gain margins is given by

$$GM_\ell = \frac{1-\delta}{1+\delta}, \; GM_u = \frac{1+\delta}{1-\delta} \tag{28}$$

as well the lower and upper disk phase margins limits as

$$PM_\ell = -2\cot(\delta), PM_u = 2\cot(\delta). \tag{29}$$

From Figures 12 and 13, the ∞ norm values of the sensitivities functions $\mathbb{S}$ and $\mathbb{T}$ for each output-feedback controller can be obtained through the peaks gains. Then using the equation (27), an upper bound δ for the uncertainty can be found and, consequently, the disk margins. For centralized LQ controller, we get

$$GM \in [-32.91, 32.91], \; PM \in [-80.94^\circ, 80.94^\circ] \tag{30}$$

while the decentralized LQ controller obtained

$$GM \in [-22.32, 22.32], \; PM \in [-99.08^{\circ}, 99.08^{\circ}]. \tag{31}$$

It can be seen that both disk margins result in a nice robustness for the closed-loop system, but the centralized design achieved a better distance for the critical point.

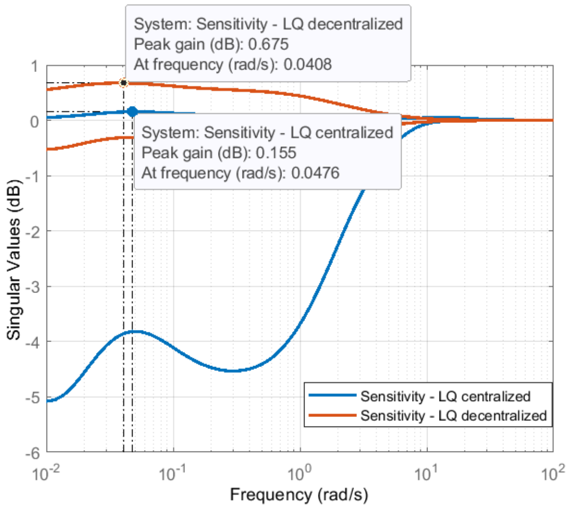

Figure 12 – Sensitivity function.

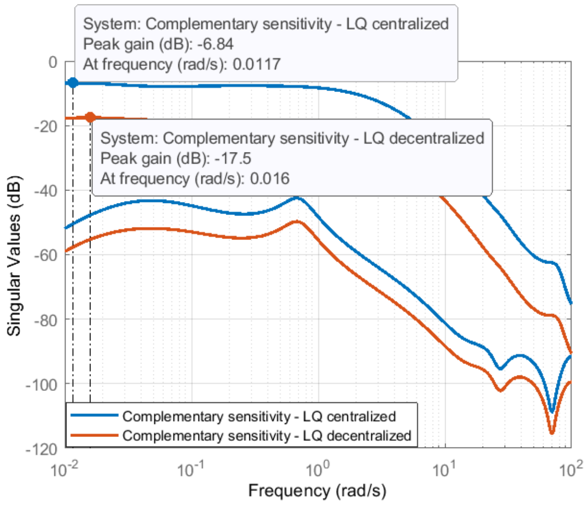

Figure 13 – Complementary sensitivity function.

5. Conclusions

In this paper, realistic designs of stability augmentation systems for the X-HALE flexible aircraft using LQ output-feedback controllers were addressed. The proposed synthesis conditions employed a set of LMIs to obtain centralized and decentralized LQ output-feedback controllers. Such conditions rely on using a single Lyapunov function and W-problem to generate sufficient LQ conditions for both structures. Simulations were performed to evaluate the stability and performance of the SAS designs. In these simulations, the closed-loop results are compared and a robustness analysis is made. As illustrated, the proposed design conditions for stability augmentation systems achieved satisfactory results. Finally, in future steps of this research, the idea is to validate such strategies in terms of nonlinear simulations or in-flight tests, as well as use different design formulations that may lead to less conservative results.

6. Contact Author Email Address

The authors' contact e-mails are: renanrlp@ita.br, pedro.gonzalez@dlr.de and flavio.silvestre@tu-berlin.de

7. Acknowledgments

This work was supported by FAPESP under grants 2019/20960-5. Moreover, the authors would like to thank Prof. Antonio Bernardo Guimarães Neto for providing the X-HALE model and comments that contributed to improve the paper.

8. Copyright Statement

References

[1] J. Theis, *Robust and Linear Parameter-Varying Control of Aeroservoelastic Systems*. PhD Dissertation: Hamburg University of Technology, 2018.

[2] T. de Souza Siqueira Versiani, F. J. Silvestre, A. B. Guimarães Neto, D. A. Rade, R. G. Annes da Silva, M. V. Donadon, R. M. Bertolin, and G. C. Silva, "Gust load alleviation in a flexible smart idealized wing," *Aerospace Science and Technology*, vol. 86, pp. 762–774, 2019.

[3] R. M. Bertolin, A. B. Guimarães Neto, G. C. Barbosa, J. A. Paulino, and F. J. Silvestre, "Design of stability augmentation systems for flexible aircraft using projective control," *Journal of Guidance, Control, and Dynamics*, vol. 44, no. 12, pp. 2244–2262, 2021.

[4] C. E. S. Cesnik, P. J. Senatore, W. Su, E. M. Atkins, and C. M. Shearer, "X-hale: A very flexible unmanned aerial vehicle for nonlinear aeroelastic tests," *AIAA Journal*, vol. 50, no. 12, pp. 2820–2833, 2012.

[5] R. Gadient, E. Lavretsky, and K. Wise, *Very Flexible Aircraft Control Challenge Problem*. AIAA Guidance, Navigation, and Control Conference, 2012.

[6] P. J. González, F. J. Silvestre, M. d. F. V. Pereira, Z. Y. Pang, and C. E. S. Cesnik, "Loop-separation control for very flexible aircraft," *AIAA Journal*, vol. 58, no. 9, pp. 3819–3834, 2020.

[7] D. Drewiacki, F. J. Silvestre, and A. B. Guimarães Neto, "Influence of airframe flexibility on pilot-induced oscillations," *Journal of Guidance, Control, and Dynamics*, vol. 42, no. 7, pp. 1537–1550, 2019.

[8] G. C. Barbosa, R. M. Bertolin, J. A. Paulino, A. B. Guimarães Neto, and F. J. Silvestre, "Design and flight test of a stability augmentation system for a flexible aircraft," *Journal of Guidance, Control, and Dynamics*, pp. 1–15, 2022.

[9] B. L. Stevens, F. L. Lewis, and E. N. Johnson, *Aircraft control and simulation: dynamics, controls design, and autonomous systems*. India: John Wiley Sons, 2015.

[10] J. A. Nelder and R. Mead, "A Simplex Method for Function Minimization," *The Computer Journal*, vol. 7, no. 4, pp. 308–313, 1965.

[11] A. B. Guimarães Neto, G. Barbosa, J. Paulino, B. R., N. J., G. P., F. Cardoso-Ribeiro, M. M., d. S. R., and B. F., "Flexible aircraft simulation validation with flight test data," *AIAA Journal*, pp. 1–20, 2021.

[12] S. Boyd, L. El Ghaoui, E. Feron, and V. Balakrishnan, *Linear Matrix Inequalities in System and Control Theory*. Society for Industrial and Applied Mathematics, 1994.

[13] C. Scherer and S. Weiland, *Linear Matrix Inequalities in Control*. NY, USA: Springer-Verlag, 2000.

[14] A. G. Neto, *Flight dynamics of flexible aircraft using general body axes: a theoretical and computational study*. Ph.D. thesis: Instituto Tecnológico de Aeronáutica, 2014.

[15] A. B. Guimarães Neto, R. G. A. Silva, P. Paglione, and F. J. Silvestre, "Formulation of the flight dynamics of flexible aircraft using general body axes," *AIAA Journal*, vol. 54, no. 11, pp. 3516–3534, 2016.

[16] E. Albano and W. P. Rodden, "A doublet-lattice method for calculating lift distributions on oscillating surfaces in subsonic flows." *AIAA Journal*, vol. 7, no. 2, pp. 279–285, 1969.

[17] W. Eversman and A. Tewari, "Consistent rational-function approximation for unsteady aerodynamics," *Journal of Aircraft*, vol. 28, no. 9, pp. 545–552, 1991.

[18] R. L. Pereira, K. H. Kienitz, and F. H. Guaracy, "Discrete-time static H_∞ loop shaping control via LMIs," *Journal of the Franklin Institute*, vol. 354, no. 5, pp. 2157–2166, 2017.

[19] B. D. O. Anderson and J. B. Moore, *Optimal control: linear quadratic methods*. Courier Corporation, 2007.

[20] C. Olalla, R. Leyva, A. El Aroudi, and I. Queinnec, "Robust LQR control for PWM converters: An LMI approach," *IEEE Transactions on Industrial Electronics*, vol. 56, no. 7, pp. 2548–2558, 2009.

[21] V. Syrmos, C. Abdallah, P. Dorato, and K. Grigoriadis, "Static output feedback—A survey," *Automatica*, vol. 33, no. 2, pp. 125–137, feb 1997.

[22] M. S. Sadabadi and D. Peaucelle, "From static output feedback to structured robust static output feedback: A survey," *Annual Reviews in Control*, vol. 42, pp. 11–26, 2016.

[23] J. Geromel and J. Bernussou, "Optimal decentralized control of dynamic systems," *Automatica*, vol. 18, no. 5, pp. 545–557, 1982.

[24] E. Feron, V. Balakrishnan, S. Boyd, and L. El Ghaoui, "Numerical methods for H_2 related problems," in *1992 American Control Conference*, 1992, pp. 2921–2922.

[25] C. A. R. Crusius and A. Trofino, "Sufficient LMI conditions for output feedback control problems," *IEEE Transactions on Automatic Control*, vol. 44, no. 5, pp. 1053–1057, 1999.

[26] E. Prempain and I. Postlethwaite, "Static output feedback stabilisation with H_∞ performance for a class of plants," *Systems Control Letters*, vol. 43, no. 3, pp. 159–166, 2001.

[27] J. Löfberg, "YALMIP: A toolbox for modeling and optimization in MATLAB," in *Proc. IEEE International*

Conference on Robotics and Automation, Taipei, Taiwan, 2004, pp. 284–289.

[28] J. F. Sturm, "Using SeDuMi 1.02, a MATLAB toolbox for optimization over symmetric cones," *Optimization Methods and Software*, vol. 11, no. 1-4, pp. 625–653, 1999.

[29] A. Schug, P. Seiler, and H. Pfifer, "Robustness Margins for Linear Parameter Varying Systems," *Aerospace Lab*, no. 13, pp. pages 1–9, Nov. 2017.